Published in final edited form as:

Circulation. 2016 August 9; 134(6): 486–498. doi:10.1161/CIRCULATIONAHA.115.021165.

Adenosine-Induced Atrial Fibrillation: Localized Reentrant Drivers in Lateral Right Atria due to Heterogeneous Expression of Adenosine A1 Receptors and GIRK4 Subunits in the Human Heart

Ning Li, MD, PhD[1,2], **Thomas A. Csepe, BS**[1,2], **Brian J. Hansen, BS**[1,2], **Lidiya V. Sul**[1,2], **Anuradha Kalyanasundaram, PhD**[1,2], **Stanislav O. Zakharkin, PhD**[1], **Jichao Zhao, PhD**[3], **Avirup Guha, MD**[1,4], **David R. Van Wagoner, PhD**[5], **Ahmet Kilic, MD**[2,4,6], **Peter J Mohler, PhD**[1,2,4], **Paul ML Janssen, PhD**[1,2,4], **Brandon Biesiadecki, PhD**[1,2], **John D Hummel, MD**[2,4,6], **Raul Weiss, MD**[2,4,6], and **Vadim V. Fedorov, PhD**[1,2]

[1]Department of Physiology & Cell Biology, The Ohio State University Wexner Medical Center, Columbus, OH, USA [2]Davis Heart & Lung Research Institute, The Ohio State University Wexner Medical Center, Columbus, OH, USA [3]Auckland Bioengineering Institute, The University of Auckland, Auckland, New Zealand [4]Department of Internal Medicine, The Ohio State University Wexner Medical Center, Columbus, OH, USA [5]Department of Molecular Cardiology, Cleveland Clinic, Cleveland Ohio, USA [6]Department of Surgery, Division of Cardiac Surgery, Wexner Medical Center, The Ohio State University, Columbus, OH

Abstract

Background—Adenosine provokes atrial fibrillation (AF) with a higher activation frequency in right atria (RA) versus left atria (LA) in patients, but the underlying molecular and functional substrates are unclear. We tested the hypothesis that adenosine-induced AF is driven by localized reentry in RA areas with highest expression of adenosine A1 receptor (A1R) and its downstream GIRK channels ($I_{K,Ado}$).

Methods—We applied bi-atrial optical mapping and immunoblot mapping of various atrial regions to reveal the mechanism of adenosine-induced AF in explanted failing and non-failing human hearts (n=37).

Results—Optical mapping of coronary-perfused atria (n=24) revealed that adenosine perfusion (10–100μM) produced more significant shortening of action potential durations (APD_{80}) in RA (from 290±45ms to 239±41ms, 17.3±10.4%; $p<0.01$) than LA (from 307±24ms to 286±23ms, 6.7±6.6%; $p<0.01$). In ten hearts, adenosine induced AF (317±116 sec) that, when sustained (≥2 min), was primarily maintained by one/two localized reentrant drivers in lateral RA. Tertiapin (10–100nM), a selective GIRK channel blocker, counteracted adenosine-induced APD shortening and

Address for correspondence: Vadim V. Fedorov, PhD, Department of Physiology and Cell Biology, The Ohio State University Wexner Medical Center, 300 Hamilton Hall, 1645 Neil Avenue, Columbus OH 43210-1218, tel: 1-614-292-9892 fax: 1-614-292-4888, vadim.fedorov@osumc.edu, fedorov.2@osu.edu.

Conflict of Interest Disclosures: None.

prevented AF induction. Immunoblotting showed that the superior/middle lateral RA had significantly higher A1R (2.7±1.7 fold; $p<0.01$) and GIRK4 (1.7±0.8 fold; $p<0.05$) protein expression than lateral/posterior LA.

Conclusions—This study revealed a three-fold RA-to-LA A1R protein expression gradient in the human heart, leading to significantly greater RA vs. LA repolarization sensitivity in response to adenosine. Sustained adenosine-induced AF is maintained by reentrant drivers localized in lateral RA regions with the highest A1R/GIRK4 expression. Selective atrial GIRK channel blockade may effectively treat AF during conditions with increased endogenous adenosine.

Keywords

adenosine; atrial fibrillation; adenosine A1 receptor; tertiapin; GIRK channel; optical mapping

Introduction

Adenosine is an endogenous nucleoside[1, 2] that is commonly used in the diagnosis and treatment of supraventricular tachyarrhythmias[3–5]. However, intravenous adenosine administration may provoke spontaneous or pacing-induced AF in up to 12–16%[6,7] of patients at clinically-relevant doses. Moreover, endogenous production of adenosine during metabolic stress conditions (e.g. ischemia[8, 9] and heart failure[10, 11]) has been suggested as a trigger of AF. In clinical and animal model studies[6, 7, 12, 13], adenosine was shown to shorten atrial action potential duration (APD) and refractoriness that could in turn provoke AF. However, the specific functional and molecular mechanisms of adenosine-induced AF, specifically in the human heart, are yet to be resolved.

Several clinical studies directly link endogenous adenosine and AF by showing that AF occurrence after acute myocardial infarction[8] and coronary artery bypass graft[9] may be treated by blockade of adenosine receptors. At a cellular level, adenosine has been shown to induce atrial APD shortening mainly through activation of specific G protein–coupled adenosine A1 receptors (A1R) and the downstream outward potassium channel $I_{K,Ado}$ formed by GIRK1 and GIRK4 subunits[1, 14–16]. Based on these findings, selective inhibition of $I_{K,Ado}$ may prevent adenosine-induced pro-fibrillatory APD shortening and AF; however, this hypothesis has never been evaluated in human atria.

Moreover, two clinical studies[17, 18] have proposed that the magnitude of adenosine's effect on repolarization/refractoriness is greater in the right atrium (RA) compared to the left atrium (LA), indicating that a gradient of sensitivity might exist across the atria. However, the molecular mechanisms that cause the heterogeneous effect of adenosine across the human atria are unknown. A limited number of studies have explored GIRK1 and GIRK4 channel expression and function through acetylcholine-mediated effects ($I_{K,ACh}$) in human hearts[19–22], but they were restricted to using right and/or left atrial appendage tissue, which are not typical arrhythmogenic regions for AF[23, 24]. Currently, no data exist regarding expression, localization, and functional contribution of A1R and adenosine-mediated activation of GIRK channels ($I_{K,Ado}$) to adenosine-induced AF across multiple regions of the human atria and particularly in the regions that are prone to AF drivers such as the posterior LA and lateral RA[23, 24].

In the present study, we used high-resolution bi-atrial optical mapping[25, 26] of human atria combined with detailed regional molecular mapping of A1R and GIRK expression across ten regions of the RA and LA to address the functional and molecular mechanisms of adenosine-induced AF. We specifically compared human RA and LA sensitivities to adenosine and evaluated the correlation of regional A1R and GIRK protein expression across the RA and LA with AF initiation. Our study reveals that expression of A1R and GIRK4 protein are higher in the human RA, specifically in the superior lateral region, that directly correlate with the source of AF maintenance by one/two localized reentrant drivers. We further show that the selective GIRK channel blocker tertiapin[27] successfully terminated and prevented AF, suggesting that the arrhythmogenic effect of adenosine in the human atria is mediated by activation of GIRK channels. Based on our results, specific blockade of the GIRK channels may offer a novel mechanism to prevent adenosine-mediated AF in the human heart.

Methods

An expanded Material and Methods section can be found in the Supplemental Material.

Patient Groups

De-identified, coded human hearts (n=37) were obtained from The Ohio State University Cardiac Transplant Team and LifeLine of Ohio Organ Procurement Organization. This study was approved by The Ohio State University Institutional Review Board. Human atrial tissue was utilized for optical mapping experiments (n=24) and/or immunoblotting analysis (n=18). Patient-specific data are presented in Supplemental Tables I–II. Six digit de-identified case numbers are presented in parentheses after heart number.

Optical Mapping of Coronary-Perfused Human Atrial Preparations

Human atrial preparations (n=24) were isolated and coronary-perfused as previously described[25, 26, 28]. The atrial preparations were immobilized with 10μM blebbistatin and stained with near-infrared dye di-4-ANBDQBS (10–40μM)[29]. Imaging was simultaneously conducted with two to four MiCAM Ultima-L CMOS cameras (SciMedia, Ltd., CA USA) from atrial epicardial (Figure 1) and/or endocardial (Figure 2) fields of view (330–940 mm^2 resolution, 100×100 pixels), sampled at 1000 frames/s.

Atrial preparations (n=19) were sequentially imaged during perfusion by regular Tyrode's solution (baseline), 10μM and/or 100μM adenosine (Sigma MO, USA) followed by the selective GIRK channel blocker tertiapin (10–100nM) (Tocris, Bristol, UK) or washout. In five preparations, 100μM adenosine was added after 100nM tertiapin perfusion. The time interval between drug applications was 20–30 minutes. All preparations were paced at a basic cycle length (CL) of 500ms, and paced incrementally until the functional refractory period was reached or AF was induced[26, 28]. Burst pacing with a CL faster than functional refractory period was also used to induce AF.

Optical mapping data were analyzed using a customized Matlab program as previously described[12, 26]. Atrial activation patterns and 80% of repolarization (APD80) were analyzed during baseline, adenosine, and tertiapin perfusion. Activation frequency of RA and LA

during AF was measured with dominant frequency (DF) analysis and discrete islands of highest DF were considered AF driver regions, which were limited to 2.5×2.5cm^2 regions[25, 26](Figure 3–5). Additionally, activation maps (Figures 3–5) were used to identify the mechanism of AF reentrant drivers as done previously[26]. Here, AF drivers are defined as a localized source(s) of fastest electrical activity visualized as reentrant circuits where two pivot points were mapped or breakthrough pattern and incomplete reentry circuits where one pivot point was mapped. These drivers were temporally stable for more than 70% of AF duration if only one driver or >30% if two drivers. The temporal stability of the AF driver is estimated by the percentage of activation cycles with activation source origin within a driver region during an 8 second recording. Based on our previous transmural mapping study[26], we suggest that the incomplete reentry or stable breakthrough visualized in the present study by single-sided mapping is intramural reentry, and this pattern is referred to as incomplete reentry/breakthrough (Supplemental Figure I). Breakthroughs distributed within 1×1 cm^2 area of the driver region during an AF episode are defined as spatially stable breakthroughs. Breakthroughs distributed between 1×1cm^2 and 2.5×2.5cm^2 area of the driver region are defined as spatially unstable breakthroughs. Detailed methods for optical mapping and data analysis are provided in the Supplemental Material.

Immunoblotting

Fresh atrial tissue (n=13) was collected from different atrial locations (as shown in Figure 6) to study the A1R and GIRK1/4 protein expression. Detailed methods for protein isolation and immunoblotting are provided in the Supplemental Material.

Statistical Analysis

Data are presented as mean ± SD other than AF episode duration, which is presented as mean ± SEM. P-values of 0.05 or below were considered significant. Additional methods for statistical analysis are provided in the Supplemental Material.

Results

Adenosine Induces Heterogeneous Action Potential Duration Shortening

RA vs LA APD comparisons were obtained from bi-atrial epicardial (n=9) or endocardial (n=2) mapping experiments during 500ms CL pacing. At baseline, average APD was similar in RA vs. LA (281±49ms vs 310±22ms, p=0.10, n=11). Adenosine perfusion induced heterogeneous APD shortening, as shown in Figures 1–2. Maximal APD shortening occurred after 2–5 minutes of adenosine perfusion. APD shortening from baseline to adenosine 10μM perfusion was significantly greater in RA than LA (17.4±11.7% vs 6.3±5.5%, p=0.02, n=11). Adenosine 100μM perfusion did not significantly shorten APD further (Figure 1C). In all RA and/or LA preparations (n=23), adenosine perfusion (10–100μM) produced greater APD shortening in RA (from 290±45ms to 239±41ms, 17.3±10.4%, p<0.01 n=21) than LA (from 307±24ms to 286±23ms, 6.7±6.6%, p<0.01 n=13). The APD shortening induced by 10μM and 100μM adenosine perfusion decreased the functional refractory period in lateral RA (n=19) from 232±60ms (baseline) to 199±56ms with 10μM adenosine (p<0.05 vs baseline) and 171±58ms with 100μM adenosine (p<0.01 vs. baseline). Simultaneous dual-sided mapping experiments showed that 100μM

adenosine-induced APD shortening was similar in epicardial (17.2±7.8%) and endocardial (16.8±7.4%) atrial layers in both RA and LA. No significant difference in APD shortening in response to adenosine was detected between failing vs. non-failing groups (Supplemental Table III).

To confirm that the observed functional changes were due to adenosine-activated $I_{K,Ado}$ current, 50–100nM tertiapin was added following adenosine perfusion (n=12). Tertiapin completely reversed the adenosine-induced APD shortening. Importantly, in five preparations tertiapin addition at baseline caused insignificant APD changes (from 310±40ms at baseline to 317±31ms, p=0.75) and subsequent addition of 100μM adenosine did not significantly shorten APD in comparison to baseline (302±35ms, p=0.74). Figure 1C shows the average APD of different atrial regions (RA vs. LA) at baseline, and during adenosine and tertiapin perfusion. Neither adenosine nor tertiapin had a significant effect on either RA or LA activation patterns (Figures 1–2).

Adenosine Induces Sustained AF with Localized Reentrant Drivers in Right Atria

At baseline, burst pacing at rates up to the functional refractory period induced non-sustained AF episodes (duration of 16±9s) in only three intact atrial preparations. Adenosine significantly increased AF inducibility and duration; burst pacing induced AF in 5 preparations (duration of 241±143s, p=0.03 vs. baseline, 3/5 sustained AF) at 10μM adenosine and in 9 preparations (duration of 222±74s, p=0.02 vs. baseline, 5/9 sustained AF) at 100μM adenosine. Addition of tertiapin (n=8) terminated adenosine-induced AF and/or prevented its reinduction (Figure 3A). After 15 minutes of tertiapin perfusion, only one non-sustained AF episode (30s) was induced in one preparation where AF (88s) was induced at baseline.

During adenosine-induced AF, the average DF in the RA was higher than LA (8.2±2.7Hz vs. 4.8±1.2Hz, p<0.01) and the maximal DF was also greater in RA than LA (9.6±3.1Hz vs 6.2± 2.3Hz p<0.01). Figures 3–5 show that the maximal DF was localized to the region of shortest APD during adenosine perfusion (see Figures 1–2). This was a consistent observation for all AF-inducible atrial preparations (n=10).

In the regions of maximal DF during sustained AF (duration ≥2min), one or two localized drivers were identified in the pectinate muscle network of the lateral RA (Supplemental Figures II–III). Localized AF drivers were seen as complete reentry circuits in 3 hearts (Figure 4 and Figure 5) and incomplete reentry circuits/breakthrough in 7 hearts (Figure 3 and Supplemental Figure I). Specific characteristics of AF drivers are given in Table 1. The size of the complete reentry circuits and the average conduction velocity around the driver circuit were measured as shown in Supplemental Figure III–IV. The average size of complete reentry circuits was 18.5±8.4mm × 6.7±2.5mm. Complete reentrant circuits and stable breakthroughs were observed during 8 episodes of adenosine-induced AF in 6 hearts. In these 6 hearts, the APD80 of the AF driver regions (n=8) was shorter than that of the driver regions (n=4) with unstable breakthroughs in the other 4 hearts (177±37ms vs 235±15ms, P<0.05). Additionally, the APD80 of the AF driver regions in 8 sustained AF episodes was shorter than the driver regions in 5 non-sustained AF episodes (181±40ms vs

225±24ms, P<0.05, Supplemental Figure VA). Figure 6 shows AF characteristics including driver locations and stability for all ten hearts.

Figure 6B–D shows APD dispersion across the atria in AF inducible vs. non-inducible preparations. No differences in APD values or APD dispersions were found between groups at baseline. However, during adenosine perfusion, AF-inducible hearts exhibited more pronounced APD shortening in the lateral RA than non-inducible hearts (23±11%, n=10 vs 13±8%, n=11, p=0.03) at 500ms pacing. AF inducibility during adenosine perfusion required short APD values (206±44ms vs 245±34ms in non-inducible hearts, p=0.04) (Figure 6C) and high APD dispersion in the RA (Figure 6D). Figure 6E shows greatest APD shortening in AF driver regions compared to other atrial regions. Importantly, the highest DF had a strong inverse correlation with APD in the driver region (r^2=0.76, p<0.01, Supplemental Figure VB).

A1R and GIRK4 Protein Expression is Higher in Right versus Left Atria

Adenosine A1R and the two main cardiac subunits of the $I_{K,Ado}$ channel protein (GIRK1 and GIRK4) were analyzed in ten different regions across the atria. Figure 7A shows that A1R and GIRK4 proteins were most highly expressed in the superior lateral RA tissue isolated from the region of maximum APD shortening (Figure 2B) and the reentrant AF driver location (Figure 4). Figure 7B shows immunoblotting results from non-mapped donor Heart #30, which also exhibited higher A1R and GIRK4 protein expression in the superior-middle lateral RA vs. other atrial regions. However, GIRK1 protein expression was similar in lateral RA vs. LA, a consistent observation in other hearts. Figure 7C summarizes A1R and GIRK4 protein expression in six representative atrial regions from both failing and non-failing hearts (n=14). Molecular mapping revealed significantly higher A1R (2.7±1.7 fold; p<0.01) and GIRK4 (1.7±0.8 fold; p<0.05) protein expression in the superior-middle lateral RA (main adenosine-induced AF driver locations) vs. lateral and posterior LA (Figure 7C). Moreover, the RA/LA protein expression ratio of A1R and GIRK4 were compared across diseases of HF and AF; however, the protein expression ratios were not significantly different between groups (Supplemental Figure VI).

Discussion

In this study, integration of optical mapping and regional immunoblot analysis allowed us to resolve the functional and molecular mechanisms underlying adenosine-induced AF in the *ex vivo* human atria. The major findings of the study are: expression of A1R and GIRK4 protein is heterogeneous across the human atria and is highest in the superior lateral region of the right atria; adenosine induced heterogeneous APD shortening and increased the incidence of AF; during adenosine-induced AF, DF was higher in the RA than LA, and regions of highest DF correspond to regions of highest A1R and GIRK protein expression in the RA; the direct correlation of AF driver location to location of both shortest APD and highest A1R and GIRK4 protein expression in the lateral RA reveals the mechanism of adenosine-induced AF.

Right and Left Atrial Differences of Adenosine Sensitivity Predisposes AF Drivers to the Right Atria

In our human atria *ex vivo* optical mapping experiments, atrial repolarization times analyzed during 500ms pacing at baseline in RA (290±45ms) and LA (307±24ms) were within the range of clinical monophasic action potential measurements of RA (209–351ms) and LA (202–339ms) in patients with and without AF history[18, 30]. Tebbenjohanns et al[6] previously reported that intravenous bolus of 6mg and 12mg adenosine induced 19% and 27% APD shortening at 500ms pacing in RA, which is comparable to our *ex vivo* findings (Figures 1–2).

Our observation of an RA-to-LA gradient of adenosine-induced APD shortening in the human heart is supported by clinical studies of adenosine's effect on AF DF in RA and LA[17, 18, 31], as DF values can represent the local functional refractoriness of the tissue[17]. We observed higher DF in lateral RA vs. LA (9.6 ±3.1Hz vs. 6.2±2.3Hz) during adenosine-induced AF. (Figures 3–5). In a similar pattern, the clinical study by Botteron et al[17] showed that a bolus of 12mg adenosine during paroxysmal or pacing-induced AF dramatically increased DF more in the lateral RA (6.4±0.7Hz to 12.2±1.9Hz) than LA (6.1±0.6Hz to 8.7±1.2Hz). Importantly, the high RA DF values (9.6±3.1Hz) in our study are in range of DF values reported by this (12.2±1.9Hz)[17] and other clinical AF studies[32,33].

Although a LA-to-RA DF gradient commonly exists in paroxysmal AF[31], a recent clinical study reported that some AF patients may have a RA-to-LA DF gradient[34]. Moreover, adenosine triphosphate injection was also shown to augment this RA-to-LA DF gradient by predominantly increasing the DF in the superior RA vs. LA (10.7±0.7Hz vs 7.9±1.8Hz)[34]. Atienza et al[31] reported that adenosine increased DF in RA more than LA in persistent AF patients. These clinical observations[6, 7, 17, 18, 31] of a greater DF increase in the superior lateral RA vs LA suggest a more pronounced adenosine-induced atrial repolarization and refractoriness in RA vs. LA. These *in vivo* findings are supported by our *ex vivo* observations that highest DF during adenosine-induced AF was always located in the shortest APD region in lateral RA (Figures 3–5, Supplemental Figure V).

Mechanism of Adenosine-induced AF

The direct effect of adenosine on cardiomyocytes is activation of the outward potassium (K+) current, I_{KAdo}, via activation of the G_i protein-coupled A1R[1]. I_{KAdo} channels are also regulated by the neurotransmitter acetylcholine (ACh) via M_2 muscarinic receptors, referred to as I_{KACh}[15, 16]. Augmented (endogenous or external) adenosine as well as vagal nerve stimulation readily promotes AF induction and maintenance due to accelerated atrial repolarization and shortened atrial refractoriness as a consequence of the activation of the GIRK current ($I_{KAdo/ACh}$)[17, 20].

Clinical studies[31, 34] have suggested the presence of AF reentrant drivers localized in the RA during adenosine infusion, but the direct mechanism sustaining AF was not shown. In this study, we have located areas of highest DF in the lateral RA during adenosine-induced AF and resolved in these regions that localized reentrant drivers may sustain AF (Figures 3–5). We observed that sustained adenosine-induced AF may be driven by one to two localized

reentry circuits, but during non-sustained AF, only unstable reentries/breakthroughs were observed in the areas of highest DF. These observations are in agreement with Schuessler et al[35, 36] canine ACh-induced AF studies that demonstrated ACh dose-dependently decreases refractory period and produces unstable AF until a critical level of refractory period, when AF becomes sustained and driven by a localized source.

Our recent dual-sided endo-epicardial optical mapping study of *ex vivo* human atria integrated with 3D gadolinium-enhanced MRI revealed that pinacidil-induced sustained AF was driven by spatially and temporally stable intramural reentry, and that targeted ablation of these reentrant tracks terminated AF[26]. The detailed 3D structural analysis in that study[26] showed pectinate muscles and areas of disorganized myofiber orientation between the endo- and epicardium create microanatomic tracks that stabilize reentrant AF drivers. Supplemental Figure II shows the endocardial pectinate muscles anatomy that may harbor a reentrant track that was only partially seen from the sub-epicardial mapping. Supplemental Figure III shows the full sub-endocardial microanatomic track revealed by 3D micro-CT. Importantly, these microanatomic tracks often involve both the sub-endo- and sub-epicardial myocardial layers. The simultaneous dual-sided electrode mapping in the canine ACh-induced AF model[36] also revealed that the reentrant pathways could be outside of the epicardial or endocardial plane and the reentry activation could appear in a stable breakthrough pattern on the single atrial surface. Thus, it is not surprising that single surface mapping may have only visualized part of the localized intramural reentry circuit[26] during sustained AF, and instead revealed three main patterns of how intramural drivers can be visualized: 1) complete reentry circuits with two pivoting points; 2) spatially stable breakthrough with incomplete reentry circuits where one pivoting point was mapped; and 3) spatially unstable beat-to-beat variable breakthroughs (Table 1, Figure 6, Supplementary Figure I). Therefore, once again this study suggests that in order to disclose the accurate AF mechanism, a simultaneous endo-epicardial and panoramic optical-mapping approach must be applied, which is currently impossible in the whole intact human atria.

Molecular Substrates of Right vs. Left Atrial Adenosine Sensitivity: Heterogeneous A1R and GIRK4 Distribution

Using isolated cardiomyocytes from human atrial appendages, Voigt et al[20] reported that GIRK1 and GIRK4 proteins were higher in RA vs. LA, and that carbachol-activated $I_{K,ACh}$ was 70% larger in RA vs. LA in patients in sinus rhythm[20]. However, no data have been reported on A1R distribution across the human atria. For the first time, we performed molecular mapping of A1R and GIRK1/4 proteins from multiple regions across the entire atria and directly correlated protein expression with functional mapping data. We found that, while GIRK1 protein expression level is similar in both human atria, A1R and GIRK4 channels are more highly expressed in the RA than LA (Figure 6), which is supported by clinical[17, 18, 31, 34] and our *ex vivo* functional data on RA vs. LA adenosine sensitivity. Importantly, the correlation of expression of these proteins with regions of shortest APD and AF driver locations in lateral superior/middle RA during adenosine perfusion suggests that A1R and GIRK4 expression may contribute to the molecular substrate for human AF.

A1R/GIRK4 Remodeling in Heart Failure

Heart failure causes structural and molecular remodeling in the atria as well as increased incidence of AF[37, 38]. Plasma adenosine levels increase progressively with the severity of chronic HF[10]. Recently, we reported that in the canine chronic heart failure model upregulation of A1R and GIRK4 expression in the RA is correlated with APD shortening and high occurrence of adenosine-induced AF, suggesting that an increased sensitivity of failing atria to adenosine may be a risk factor for AF in heart failure[12]. In the current study, we found A1R and GIRK4 protein expression gradients between lateral RA and LA are also highly present in hearts with history of heart failure and/or AF (Figure 7B and Supplemental Figure VI), which in combination with the elevated levels of endogenous adenosine reported in heart failure patients[11] may initiate AF with an RA-to-LA DF gradient. The variety of disease history within each group may limit the ability to show the effects of independent disease remodeling on protein expression, which requires further investigation.

Limitations

In this study, we utilized *ex vivo* atrial preparations that are unbiased to the compounding influence of the autonomic nervous system, which could have partially modulated the response to adenosine *in vivo*. The small sample size of hearts with a variety of diseases limits our ability to fully account for and make specific suggestions regarding A1 and GIRK expressions as well as AF susceptibility/inducibility for disease factors such as heart failure, hypertension, coronary heart disease and diabetes. Moreover, incomplete atria (paucity of pulmonary vein and intra-septal regions) received from transplanted failing hearts limited our statistical analysis of AF inducibility between failing vs non-failing hearts. Although the mechanism of adenosine-induced AF in explanted human hearts may also play an important role in human AF *in vivo*, its significance in persistent AF patients relative to other factors is still unclear. As we utilized primarily single-sided epicardial or endocardial mapping, we could not visualize complete reentry activation during AF in some preparations. Additionally, as we focused on estimating the antiarrhythmic efficacy of tertiapin, we did not perform targeted ablation of any of the driver areas to determine whether it would eliminate the AF. However, our previous studies support the assumption that ablation of these reentrant drivers would result in termination or significant alteration of AF[26]. Even though all AF drivers were localized in the lateral RA, we cannot exclude the possibility that adenosine-provoked AF can be maintained by a LA driver in some patient categories, as many factors can be involved in the induction and maintenance of AF.

Potential Implications and Future Directions

For the first time, our study reveals the potential molecular and functional mechanisms that may underlie adenosine-induced AF events in the human heart. Mechanistically, the high expression of the two main components (A1R and GIRK4 channels) of the adenosine signaling pathway, particularly in the superior lateral RA, correlates with the localization of reentrant drivers. Our results also indicate that all AF drivers were localized in the shortest APD regions, which suggests that in the clinical setting, adenosine injection may be a useful tool for unmasking the location of right atrial AF drivers and improving targeted ablation treatment. Interestingly, tertiapin reversed the APD shortening caused by adenosine and

prevented AF induction, confirming the potential utility of selective GIRK channel blockers in the treatment of AF in humans. The mechanism of why A1R expression is at least two-fold higher in the RA than LA in the human heart requires further evaluations.

Conclusions

We demonstrated for the first time in the human heart that a near 3-fold greater RA-to-LA A1R protein expression leads to significantly greater APD shortening in the RA vs. the LA in response to adenosine.

Highest A1R and GIRK4 expression is present in the pectinate muscle region of the superior and middle lateral RA and is correlated with the areas of greatest adenosine-induced repolarization shortening. Adenosine primarily induces AF sustained by localized reentrant drivers in the superior-middle lateral RA, where shortest APD and highest A1R expression are observed. The selective GIRK channel blocker tertiapin successfully prevents and/or terminates adenosine-induced AF, suggesting that selective blockade of cardiac GIRK channels is a potential treatment for adenosine-mediated AF.

Supplementary Material

Refer to Web version on PubMed Central for supplementary material.

Acknowledgments

We thank the Lifeline of Ohio Organ Procurement Organization and the Division of Cardiac Surgery at The OSU Wexner Medical Center for providing the explanted hearts. The human heart program repository is supported by the Davis Heart and Lung Research Institute. We thank for Mr. Benjamin Canan and Mr. Eric Schultz for their help with tissue processing.

Funding Sources

This work was supported primarily by NIH HL115580 (to VVF), and partially by CR Webb Fund in Cardiovascular Research and The OSU Heart and Vascular Center TriFit Challenge Discovery Fund (VVF), the NIH HL113084 (PMLJ), HL084583, HL083422, HL114383 (to PJM), HL114940 (to BJB) and HL111314 (to DVW).

References

1. Lerman BB, Belardinelli L. Cardiac electrophysiology of adenosine. Basic and clinical concepts. Circulation. 1991; 83:1499–1509. [PubMed: 2022011]
2. Headrick JP, Peart JN, Reichelt ME, Haseler LJ. Adenosine and its receptors in the heart: regulation, retaliation and adaptation. Biochim Biophys Acta. 2011; 1808:1413–1428. [PubMed: 21094127]
3. Camm AJ, Garratt CJ. Adenosine and supraventricular tachycardia. N Engl J Med. 1991; 325:1621–1629. [PubMed: 1944450]
4. Rankin AC, Brooks R, Ruskin JN, McGovern BA. Adenosine and the treatment of supraventricular tachycardia. [Review]. American Journal of Medicine. 1992; 92:655–664. [PubMed: 1605147]
5. Datino T, Macle L, Qi XY, Maguy A, Comtois P, Chartier D, Guerra PG, Arenal A, Fernandez-Aviles F, Nattel S. Mechanisms by which adenosine restores conduction in dormant canine pulmonary veins. Circulation. 2010; 121:963–972. [PubMed: 20159830]
6. Tebbenjohanns J, Schumacher B, Pfeiffer D, Jung W, Luderitz B. Dose and rate-dependent effects of adenosine on atrial action potential duration in humans. J Interv Card Electrophysiol. 1997; 1:33–37. [PubMed: 9869948]

7. Strickberger SA, Man KC, Daoud EG, Goyal R, Brinkman K, Knight BP, Weiss R, Bahu M, Morady F. Adenosine-induced atrial arrhythmia: a prospective analysis. Ann Intern Med. 1997; 127:417–422. [PubMed: 9312997]

8. Bertolet BD, Hill JA, Kerensky RA, Belardinelli L. Myocardial infarction related atrial fibrillation: role of endogenous adenosine. Heart. 1997; 78:88–90. [PubMed: 9290409]

9. Yavuz T, Bertolet B, Bebooul Y, Tunerir B, Aslan R, Ocal A, Ybribim E, Kutsal A. Role of endogenous adenosine in atrial fibrillation after coronary artery bypass graft. Clin Cardiol. 2004; 27:343–346. [PubMed: 15237694]

10. Funaya H, Kitakaze M, Node K, Minamino T, Komamura K, Hori M. Plasma adenosine levels increase in patients with chronic heart failure. Circulation. 1997; 95:1363–1365. [PubMed: 9118500]

11. Franceschi F, Deharo JC, Giorgi R, By Y, Monserrat C, Condo J, Ibrahim Z, Saadjian A, Guieu R. Peripheral plasma adenosine release in patients with chronic heart failure. Heart. 2009; 95:651–655. [PubMed: 19039025]

12. Lou Q, Hansen BJ, Fedorenko O, Csepe TA, Kalyanasundaram A, Li N, Hage LT, Glukhov AV, Billman GE, Weiss R, Mohler PJ, Gyorke S, Biesiadecki BJ, Carnes CA, Fedorov VV. Upregulation of adenosine A1 receptors facilitates sinoatrial node dysfunction in chronic canine heart failure by exacerbating nodal conduction abnormalities revealed by novel dual-sided intramural optical mapping. Circulation. 2014; 130:315–324. [PubMed: 24838362]

13. Kabell G, Buchanan LV, Gibson JK, Belardinelli L. Effects of adenosine on atrial refractoriness and arrhythmias. Cardiovasc Res. 1994; 28:1385–1389. [PubMed: 7954650]

14. Ip JE, Cheung JW, Chung JH, Liu CF, Thomas G, Markowitz SM, Lerman BB. Adenosine-induced atrial fibrillation: insights into mechanism. Circ Arrhythm Electrophysiol. 2013; 6:e34–e37. [PubMed: 23778252]

15. Visentin S, Wu SN, Belardinelli L. Adenosine-induced changes in atrial action potential: contribution of Ca and K currents. Am J Physiol. 1990; 258:H1070–H1078. [PubMed: 2330994]

16. Belardinelli L, Isenberg G. Isolated atrial myocytes: adenosine and acetylcholine increase potassium conductance. Am J Physiol. 1983; 244:H734–H737. [PubMed: 6846564]

17. Botteron GW, Smith JM. Spatial and temporal inhomogeneity of adenosine's effect on atrial refractoriness in humans: using atrial fibrillation to probe atrial refractoriness. J Cardiovasc Electrophysiol. 1994; 5:477–484. [PubMed: 8087292]

18. Nakai T, Watanabe I, Kunimoto S, Kojima T, Kondo K, Saito S, Ozawa Y, Kanmatsuse K. Electrophysiological effect of adenosine triphosphate and adenosine on atrial and ventricular action potential duration in humans. Jpn Circ J. 2000; 64:430–435. [PubMed: 10875733]

19. Koumi S, Arentzen CE, Backer CL, Wasserstrom JA. Alterations in muscarinic K+ channel response to acetylcholine and to G protein-mediated activation in atrial myocytes isolated from failing human hearts. Circulation. 1994; 90:2213–2224. [PubMed: 7955176]

20. Voigt N, Trausch A, Knaut M, Matschke K, Varro A, Van Wagoner DR, Nattel S, Ravens U, Dobrev D. Left-to-right atrial inward rectifier potassium current gradients in patients with paroxysmal versus chronic atrial fibrillation. Circ Arrhythm Electrophysiol. 2010; 3:472–480. [PubMed: 20657029]

21. Dobrev D, Wettwer E, Himmel HM, Kortner A, Kuhlisch E, Schuler S, Siffert W, Ravens U. G-Protein beta(3)-subunit 825T allele is associated with enhanced human atrial inward rectifier potassium currents. Circulation. 2000; 102:692–697. [PubMed: 10931811]

22. Deshmukh A, Barnard J, Sun H, Newton D, Castel L, Pettersson G, Johnston D, Roselli E, Gillinov AM, McCurry K, Moravec C, Smith JD, Van Wagoner DR, Chung MK. Left atrial transcriptional changes associated with atrial fibrillation susceptibility and persistence. Circ Arrhythm Electrophysiol. 2015; 8:32–41. [PubMed: 25523945]

23. Narayan SM, Krummen DE, Clopton P, Shivkumar K, Miller JM. Direct or coincidental elimination of stable rotors or focal sources may explain successful atrial fibrillation ablation: on-treatment analysis of the CONFIRM trial (Conventional ablation for AF with or without focal impulse and rotor modulation). J Am Coll Cardiol. 2013; 62:138–147. [PubMed: 23563126]

24. Haissaguerre M, Hocini M, Denis A, Shah AJ, Komatsu Y, Yamashita S, Daly M, Amraoui S, Zellerhoff S, Picat MQ, Quotb A, Jesel L, Lim H, Ploux S, Bordachar P, Attuel G, Meillet V, Ritter

P, Derval N, Sacher F, Bernus O, Cochet H, Jais P, Dubois R. Driver Domains in Persistent Atrial Fibrillation. Circulation. 2014; 130:530–538. [PubMed: 25028391]

25. Zhao J, Hansen BJ, Csepe TA, Lim P, Wang Y, Williams M, Mohler PJ, Janssen PM, Weiss R, Hummel JD, Fedorov VV. Integration of High-Resolution Optical Mapping and 3-Dimensional Micro-Computed Tomographic Imaging to Resolve the Structural Basis of Atrial Conduction in the Human Heart. Circ Arrhythm Electrophysiol. 2015; 8:1514–1517. [PubMed: 26671938]
26. Hansen BJ, Zhao J, Csepe TA, Moore BT, Li N, Jayne LA, Kalyanasundaram A, Lim P, Bratasz A, Powell KA, Simonetti OP, Higgins RS, Kilic A, Mohler PJ, Janssen PM, Weiss R, Hummel JD, Fedorov VV. Atrial fibrillation driven by micro-anatomic intramural re-entry revealed by simultaneous sub-epicardial and sub-endocardial optical mapping in explanted human hearts. Eur Heart J. 2015; 36:2390–2401. [PubMed: 26059724]
27. Dobrev D, Friedrich A, Voigt N, Jost N, Wettwer E, Christ T, Knaut M, Ravens U. The G protein-gated potassium current I(K,ACh) is constitutively active in patients with chronic atrial fibrillation. Circulation. 2005; 112:3697–3706. [PubMed: 16330682]
28. Fedorov VV, Glukhov AV, Ambrosi CM, Kostecki G, Chang R, Janks D, Schuessler RB, Moazami N, Nichols CG, Efimov IR. Effects of KATP channel openers diazoxide and pinacidil in coronary-perfused atria and ventricles from failing and non-failing human hearts. J Mol Cell Cardiol. 2011; 51:215–225. [PubMed: 21586291]
29. Fedorov VV, Glukhov AV, Chang R, Kostecki G, Aferol H, Hucker WJ, Wuskell JP, Loew LM, Schuessler RB, Moazami N, Efimov IR. Optical mapping of the isolated coronary-perfused human sinus node. J Am Coll Cardiol. 2010; 56:1386–1394. [PubMed: 20946995]
30. Narayan SM, Kazi D, Krummen DE, Rappel WJ. Repolarization and activation restitution near human pulmonary veins and atrial fibrillation initiation: a mechanism for the initiation of atrial fibrillation by premature beats. J Am Coll Cardiol. 2008; 52:1222–1230. [PubMed: 18926325]
31. Atienza F, Almendral J, Moreno J, Vaidyanathan R, Talkachou A, Kalifa J, Arenal A, Villacastin JP, Torrecilla EG, Sanchez A, Ploutz-Snyder R, Jalife J, Berenfeld O. Activation of inward rectifier potassium channels accelerates atrial fibrillation in humans: evidence for a reentrant mechanism. Circulation. 2006; 114:2434–2442. [PubMed: 17101853]
32. Sanders P, Berenfeld O, Hocini M, Jais P, Vaidyanathan R, Hsu LF, Garrigue S, Takahashi Y, Rotter M, Sacher F, Scavee C, Ploutz-Snyder R, Jalife J, Haissaguerre M. Spectral analysis identifies sites of high-frequency activity maintaining atrial fibrillation in humans. Circulation. 2005; 112:789–797. [PubMed: 16061740]
33. Guillem MS, Climent AM, Millet J, Arenal A, Fernandez-Aviles F, Jalife J, Atienza F, Berenfeld O. Noninvasive localization of maximal frequency sites of atrial fibrillation by body surface potential mapping. Circ Arrhythm Electrophysiol. 2013; 6:294–301. [PubMed: 23443619]
34. Hasebe H, Yoshida K, Iida M, Hatano N, Muramatsu T, Aonuma K. Right-to-left frequency gradient during atrial fibrillation initiated by right atrial ectopies and its augmentation by adenosine triphosphate: Implications of right atrial fibrillation. Heart Rhythm. 2015; 13:354–363. [PubMed: 26432585]
35. Schuessler RB, Grayson TM, Bromberg BI, Cox JL, Boineau JP. Cholinergically mediated tachyarrhythmias induced by a single extrastimulus in the isolated canine right atrium. Circ Res. 1992; 71:1254–1267. [PubMed: 1394883]
36. Schuessler RB, Kawamoto T, Hand DE, Mitsuno M, Bromberg BI, Cox JL, Boineau JP. Simultaneous epicardial and endocardial activation sequence mapping in the isolated canine right atrium. Circulation. 1993; 88:250–263. [PubMed: 8319340]
37. Thihalolipavan S, Morin DP. Atrial fibrillation and congestive heart failure. Heart Fail Clin. 2014; 10:305–318. [PubMed: 24656107]
38. Sanders P, Morton JB, Davidson NC, Spence SJ, Vohra JK, Sparks PB, Kalman JM. Electrical remodeling of the atria in congestive heart failure: electrophysiological and electroanatomic mapping in humans. Circulation. 2003; 108:1461–1468. [PubMed: 12952837]

Clinical Perspective

What is new?

- This study elucidates the molecular and functional mechanisms that may underlie adenosine-induced AF in the human heart. The integration of panoramic optical mapping and regional immunoblot allowed us to resolve that protein expression of the two main components of the adenosine signalling pathway (A1R and GIRK4) is 2–3 times higher in human right atria (RA) vs left atria (LA), leading to greater RA vs. LA action potential duration (APD) shortening in response to adenosine.
- We also found that adenosine induces AF sustained by localized reentrant drivers anchored to regions of both shortest APD and highest A1R expression in the RA.

What are the clinical implications?

- This study suggests that in the clinical setting, adenosine injection may unmask the location of right atrial AF drivers by selectively shortening APD and increasing frequency in driver regions and aid in targeted ablation treatment.
- We further demonstrated that the selective GIRK channel blocker tertiapin successfully terminated and prevented AF, suggesting that the arrhythmogenic effect of adenosine in the human atria is mediated by activation of GIRK channels. Based on our results, specific blockade of the GIRK channels may offer a novel mechanism to prevent adenosine-mediated AF in patients.

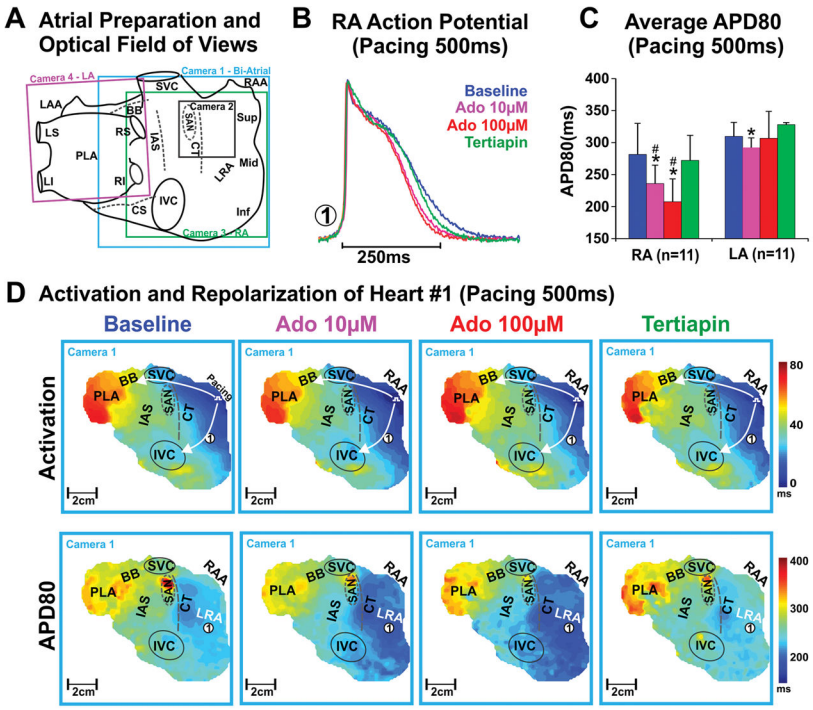

Figure 1. Epicardial optical mapping of the intact human atria

A, Schematic of the four epicardial cameras' optical fields of view. **B**, Representative optical action potential from the lateral RA (location indicated with circled #1 in panel D) of human Heart #1 (Case No. 947202). **C**, Average APD80 of RA vs LA at baseline, 10μM adenosine, 100μM adenosine and tertiapin of all bi-atrial preparations (n=11). Values are presented as mean±SD. * denotes $p<0.05$ vs baseline, # denotes $p<0.05$ vs LA. **D,** Activation (top) and APD80 (bottom) maps of Heart #1(947202) at baseline, 10μM adenosine, 100μM adenosine and 10nM tertiapin perfusion. Abbreviations: Ado – adenosine; BB – Bachmann's bundle; CS – coronary sinus; CT – crista terminalis; IAS – interatrial septum; IVC – inferior vena cava; LAA – left atrial appendages; LRA – lateral right atria; PLA – posterior left atria; RAA – right atrial appendages; SAN – sinoatrial node; SVC – superior vena cava.

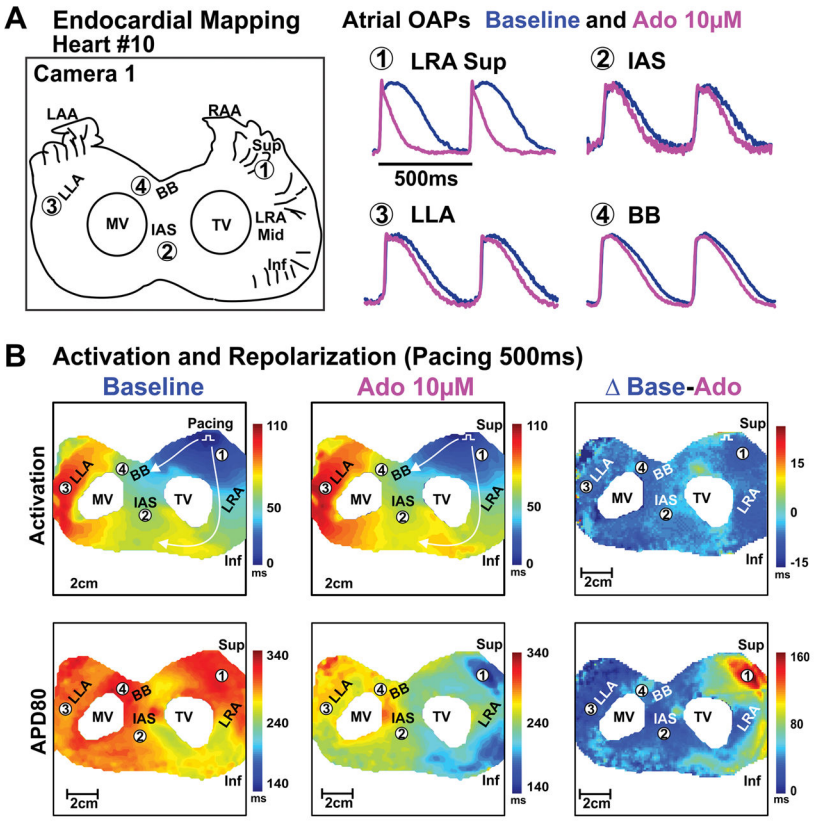

Figure 2. Endocardial optical mapping of bi-atrial preparation from failing human hearts

A, Schematic of the optical field of view and optical action potentials from different atrial regions at baseline and 10μM adenosine perfusion of human Heart #10(522421). **B,** Activation and APD80 maps of the atria at baseline and 10μM adenosine perfusion; right panel shows the differences of activation and repolarization time between baseline and adenosine perfusion. Abbreviations as in Figure 1. Inf – inferior; LLA – lateral left atria; Mid – middle; MV – mitral valve; OAP– optical action potential; Sup – superior; TV – tricuspid valve.

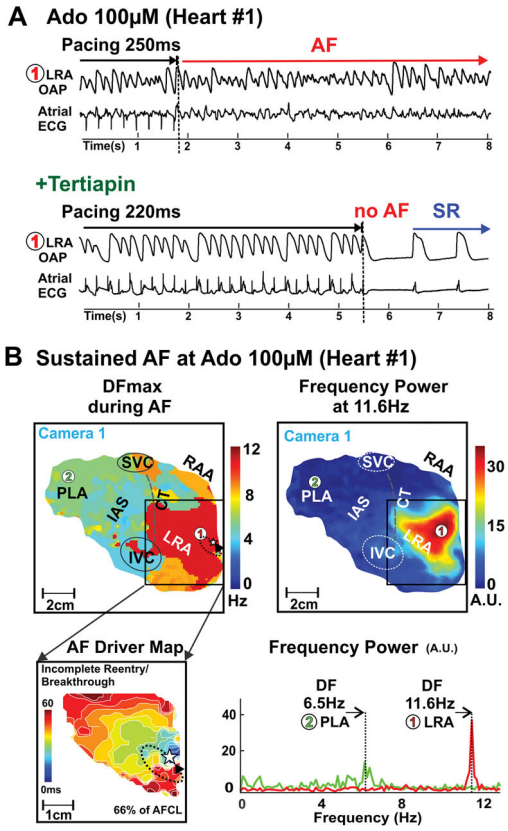

Figure 3. Adenosine-induced AF in human Heart #1(947202)

A, Atrial optical action potentials (OAPs) from location #1 and atrial ECG recordings during and after burst pacing at 100μM adenosine (top) followed by 10nM tertiapin (bottom) perfusion. **B**, Dominant frequency (top left) and frequency power map (top right) during 100μM adenosine-induced AF. Bottom left, activation map of the AF driver region. Dashed arrow shows AF driver location in region of highest DF. Star shows breakthrough location. Bottom right, Fast Fourier Transform analysis of OAPs #1 and #2 from max DF in LA and RA. AF- Atial Fibrillation; DF-Dominant frequency; SR – sinus rhythm. Abbreviations as in Figure 1.

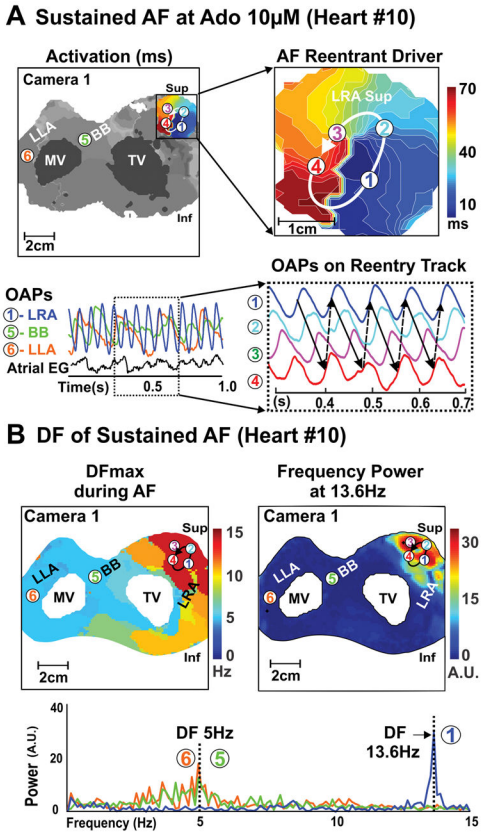

Figure 4. Optical mapping revealed a temporally and spatially stable reentrant driver in human Heart #10(522421) during 10μM adenosine-induced AF

A, Top left: Activation map of reentrant driver region during sustained adenosine-induced AF. Top right: Magnified activation map of AF reentrant driver. Bottom left: optical action potentials (OAPs 1–6) from regions across RA and LA; numbers correspond to location from top left panel. Bottom right: OAPs 1–4 showing stable reentry sustaining AF. **B**, Dominant frequency (DF) and frequency power map during this sustained AF shows greater DF and frequency power in the driver location of the RA. Abbreviations as in Figure 2.

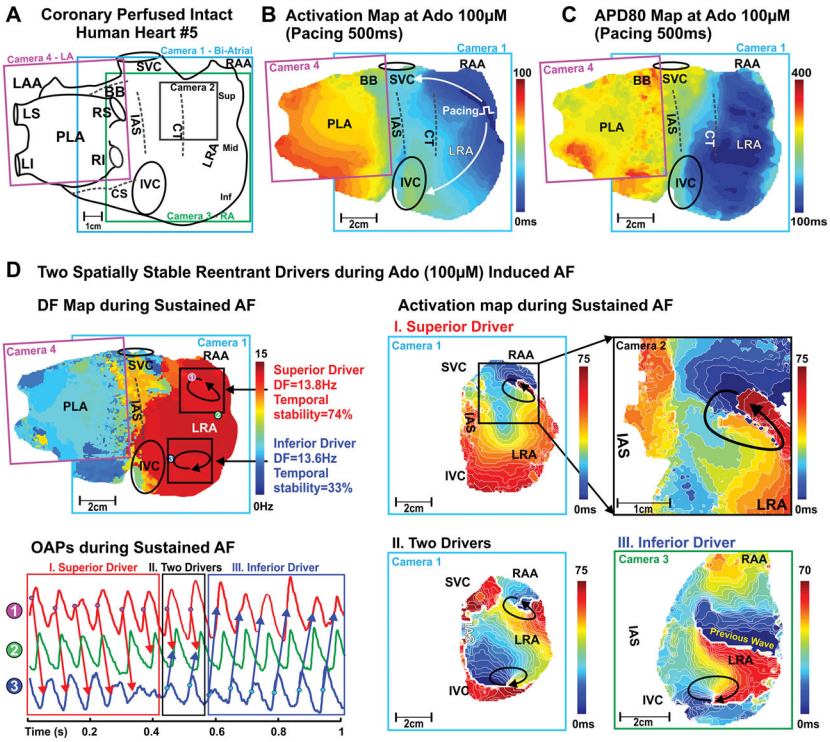

Figure 5. Optical mapping revealed two localized reentrant AF drivers in human Heart #5 (402879)

A, Schematic of the four epicardial cameras' optical fields of view. Activation map (**B**) and APD80 map (**C**) of the intact atria at pacing 500ms during adenosine 100μM. **D**, Top left: Dominant frequency (DF) map during 100μM adenosine-induced AF. Circled numbers 1–3 indicate the locations where optical action potentials (OAPs) were measured. Bottom left: OAPs from the superior (#1), inferior (#3) AF driver regions and LRA middle non-AF driver region (#2). Right: Activation maps are showing superior and inferior spatially stable AF drivers during adenosine-induced AF. Arrows indicate the location and direction of AF reentrant drivers.

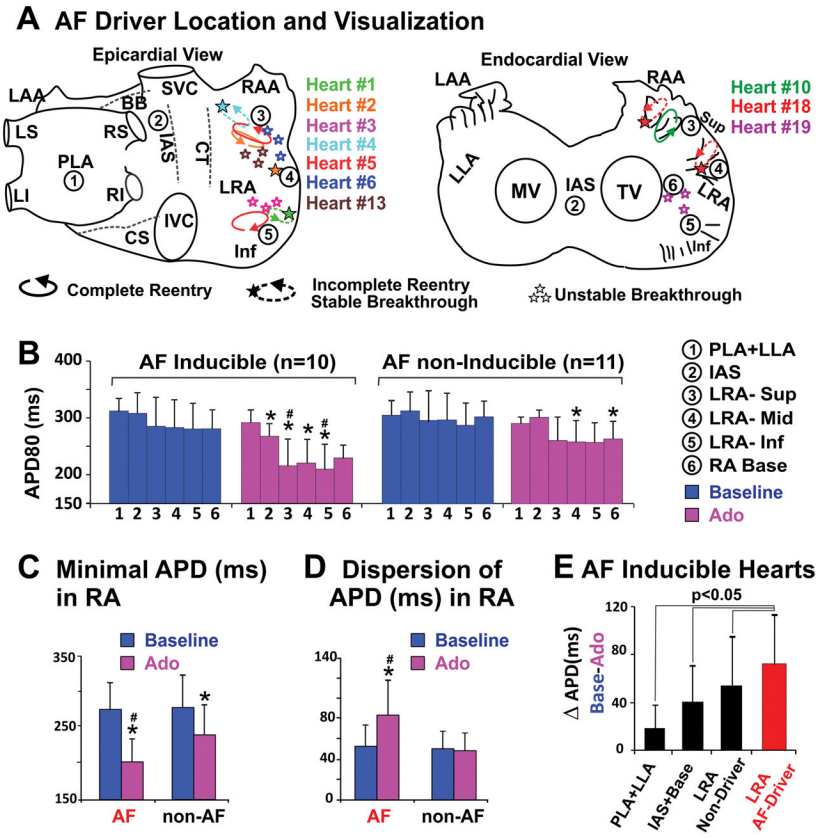

Figure 6. Distribution patterns of AF drivers and APD across the human atria

A, Locations and visualizations of AF drivers in ten AF-inducible hearts shown on epicardial and endocardial atrial schematics. Heart number is distinguished by color, and drivers from the same heart are labeled with the corresponding color. A complete reentry pattern is denoted by a complete ellipsoidal arrow; partial reentry pattern by a dashed ellipsoidal arrow. Circled numbers 1–6 indicate the regions where APD80 was measured in panel **B. B**, Average APD80 of different atrial regions in AF inducible and AF non-inducible groups at baseline and adenosine perfusion. **C–D**, Minimal APD and APD dispersion in the RA of AF inducible and AF non-inducible preparations at baseline and adenosine perfusion. **E**, APD shortening in AF driver and non-driver regions. Values are presented in mean±SD. * denotes $p<0.05$ vs baseline, # denotes $p< 0.05$ vs AF non-inducible group. Abbreviations as in Figures 1–2.

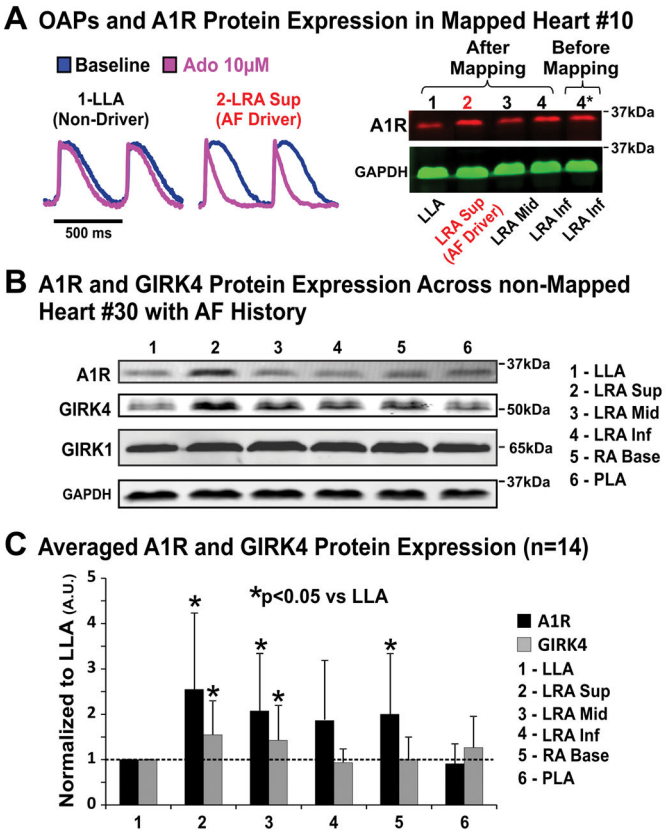

Figure 7. Molecular mapping of A1R and GIRK protein across the human atria

A, Left: optical action potentials from the superior LRA (AF driver region) and LLA (non-driver region) of Heart #10(522421). Right: A1R protein expression from the same heart after optical mapping (lanes 1–4). Lane 5* shows A1R expression from a sample collected before optical mapping of the same location as lane 4 to validate the quality of protein after optical mapping. **B**, Representative immunoblot of A1R and GIRK protein in the diseased human atria. **C**, Summary of A1R and GIRK4 protein expression in 14 human atria. GAPDH normalized band density is shown in mean±SD. Abbreviations as in Figures 1–2.

Table 1

The characteristics of AF episode in human heart

AF Characteristics					AF Driver Characteristics						
Heart No.	Condition	Duration (s)	DF(Hz)		Driver Region	DF (Hz)	CL(ms)		Stability		Visualization Type
			RA	LA			Avg	SD	Temporal	Spatial	
4	Baseline	88	5.3	4.8	RA sup	7.2	141	24	38%	unstable	BT
5	Baseline	40	5.8	4.2	RA sup	6.6	148	10	79%	stable	BT/reentry
6	Baseline	29	3.9	4.6	(1) RA sup	6.1	172	19	55%	unstable	BT
					(2) PLA	5.9	182	12	69%	unstable	BT
Unsustained adenosine-induced AF											
3	Ado 10	62	4.8	3.5	RA inf	6.0	144	48	61%	unstable	BT
3	Ado 100	63	4.1	3.4	RA inf	5.3	204	43	68%	unstable	BT
13	Ado 100	106	6.4	N/A	RA mid	7.8	121	33	64%	unstable	BT
18	Ado 100	11	7.4	N/A	(1)RA sup	8.3	128	20	81%	stable	BT/reentry
				N/A	(2)RA mid	8.3	122	10	41%	stable	BT/reentry
19	Ado 100	42	7.4	N/A	RA inf	8.1	117	31	72%	unstable	BT
Sustained adenosine-induced AF											
4	Ado 10	347	6.7	5.3	RA sup	7.2	135	28	100%	stable	BT/reentry
6	Ado 10	1173	11.6	6.5	RA sup	13.9	81	18	70%	unstable	BT
10	Ado 10	335	10.2	4.1	RA sup	13.6	74	4	100%	stable	reentry
1	Ado 100	120	8.8	5.5	RA inf	11.6	86	7	100%	stable	BT/reentry
2	Ado 100	145	8.5	4.9	RA mid	9.4	106	9	100%	stable	reentry
4	Ado 100	425	6.8	4.5	RA sup	7.5	138	27	100%	stable	BT/reentry
5	Ado 100	471	13.2	6.8	(1)RA sup	13.8	71	6	74%	stable	reentry
					(2)RA inf	13.6	72	6	33%	stable	reentry
10	Ado 100	616	11.2	3.7	RA sup	12.8	78	4	100%	stable	reentry

Abbreviations: Ado 10/100 = Adenosine 10μM/100 μM; AF = Atrial Fibrillation; APD = Action Potential Duration; BT = Breakthrough; CL = Cycle Length; DF = Dominant Frequency; LA = Left Atria; RA sup/mid/inf = Right atria superior/middle/inferior.